Determination of Phase Transformation Temperatures by Dilatometric Test of S960MC Steel

M. Málek *, M. Mičian, J. Moravec
Faculty of Mechanical Engineering, Technical University of Liberec
Studentská 1402/2, 461 17 Liberec I, Czech Republic
* Corresponding author. E-mail address: miloslav.malek@fstroj.uniza.sk

Abstract

The phenomenon of "soft zone" is occurring in the heat affected zone (HAZ) of high strength low alloy (HSLA) steels. Therefore, the process of weld metal solidification and phase transformation in HAZ is essential to understand the behaviour of the material, especially in the case where welded joints are debilitating part of the construction. The simulation program SYSWELD is powerful tool to predict solidification and phase transformation of welding joint, what correspond to the mechanical properties of the joints. To achieve relevant results of the simulation, it is necessary to use right mathematic-material model of the investigated material. Dilatometric test is the important methods to gather necessary input values for material database. In this paper is investigated physical and metallurgical properties of S960MC steel. The dilatometric curves were carried out on the laboratory machine dilatometer DIL 805L. In addition to determination of the phase transformation temperatures at eight levels of the cooling rate, the microstructure and hardness of the material are further analysed. The hardness of the samples reflects the achieved microstructure. Depending on the cooling rate, several austenitic transformation products were observed such as pearlite, bainite, martensite and many different ferritic microstructures. The differences between the transformation temperature results using the first derivation method and the three tangent method are up to 2%. The limit cooling rate was set at value 30°C/s. The microstructure consists only of bainite and martensite and the hardness reaches a value of 348HV and higher.

Keywords: Metallography, Microstructure, Dilatometry, S960MC, Transformation temperatures

1. Introduction

Welding of high-strength low-alloy steel is more difficult than common structural steel. The high tensile and yield strength of this type of steels are obtained by the combination of the chemical composition, heat treatment and the processing. The property of the joint and the welded steel can be significantly affected by the heat input of the welding process [1]. However, it has been proven by many studies, that it is possible to create a satisfactory welded joint using suitable welding technology, such as beam welding (laser and electron), laser hybrid and also advanced arc welding technology [2, 3]

High-strength steel can be achieved by the technological process of controlled rolling at high temperature and at intercritical temperature (transformation of austenite to ferrite). This technological process is called thermomechanical processing (TMCP) [4, 5, 6]. Plastic deformation and grain refinement is achieved by a TMCP process with a suitable chemical composition of steel. Microalloying elements (Nb, V, Ti) ensure

precipitation hardening and reduction of austenite grain growth. All these factors, combined with accelerated cooling, make it possible to obtain a high-strength steel with a martensite or bainite structure while maintaining a low content of carbon and alloying elements compared to a standard steel with the same mechanical properties. [1, 7].

High-strength low-alloy steels are widely used in the automotive, gas and oil industries, in the shipping industry and also in the construction of heavy machinery (large mobile crane, vehicles) [8-10]. Over the past decades, much research has been conducted on HSLA steels to examine heat treatment, phase transformations and oxidation behavior and mechanical properties. The growth of austenitic grains is significantly affected by the precipitation of microalloying elements. The more stable the precipitates, the more they can reduce growth of austenite grain at high temperature [11, 12].

The microstructure of microalloyed steel depends on many factors, such as chemical composition, cooling rate, and also the austenite grain size prior to the phase transformations. The required mechanical properties are obtained by a combination of different microstructures. Parent phase of all obtained microstructures, such as perlite, ferrite, lower or upper bainite and also martensite, is austenite [13]. The final microstructure depends on the hot rolling process, the cooling rate and also on the chemical composition [10, 12].

Continuous Cooling Transformation (CCT) diagrams describe the phase transformation in the temperature and time axes (or Log time). CCT diagram is used to predict final microstructure with their mechanical properties. In the welding process, it could help to define the microstructure obtained in the HAZ based on the cooling time, which could lead to the optimization of the welding parameters to achieve suitable joints. To avoid an undesirable complication during welding process, such as hydrogen cracks, occurring soft zones or too hard zones, which could be brittle, the CCT diagrams are used [14 - 16].

The transformation diagrams are structural diagrams, which are constructed for each steel, with specific chemical composition. Structural transformation of austenite, during cooling steel are recorded in coordinate axes temperature versus time, or temperature versus log time. Austenite transformation at steel of specific chemical composition is already described. This is useful for wide range of thermal and thermo-mechanical manufacturing [15]. CCT diagrams are usually complemented with measured values of hardness and percentage ratio of structural phases. From these diagrams, it is possible determine transformation temperatures A_{c1} and A_{c3}.

Construction of transformation diagrams are complex and expensive process, however contribution exceeds costs [15, 16]. The dilatometry analyses are one of many applicable methods for creating CCT diagrams. The dilatometry belongs to physical methods to investigate transformation changes, rate of phase transformations, coefficient of thermal expansion, position of critical temperatures of phase transformations, reversible and irreversible phase transformations [17]. It is based on recording the dimensional changes of samples affected by a controlled thermal cycle, usually with a constant heating and cooling rate. The result of the dilatometry analysis is a dilatation curve, which describes the dependence of dimensional changes on the temperature [18, 19]. The nonlinear variations at the dilatation curve indicate a phase transformation. From the above nonlinear changes, the temperature and time coordinates of the phase transformations are evaluated. All these coordinates of phase transformations are graphically recorded on the temperature and time axis, for every cooling rate [15]. The methods of three tangents or the first derivation of dilatation curve are widely used for evaluating of the nonlinear changes [20].

2. Experiments

Dilatometric analyse were used to investigate material properties of S960MC steel (Strenx 960MC – SSAB). This research investigated phase transformations of S960MC steel for different cooling rates and also research focused to specify transformation temperatures, analyse microstructure supported by hardness measurements.

2.1. Experimental material

S960MC is a TMCP steel suitable for welding and cold forming, with a minimum yield strength of 960 MPa. Strenx 960MC meets and exceeds the requirements of S960MC in EN 10149-2. The chemical compositions and mechanical properties of the investigated steel are given in the Table 1 and Table 2 according to the standard EN 10149-2 and material certificate. The investigated steel was received in the form of thermo-mechanically rolled sheets of 3 mm thickness.

Table 1.
Chemical composition of the investigated steel S960MC (wt. %)

	C	Si	Mn	P	S	Al	Nb	V	Ti	Cr	Ni	Mo
EN 10149-2	max. 0.20	max. 0.60	max. 2.20	max. 0.025	max. 0.010	min. 0.015	max. 0.090	max. 0.200	max. 0.25	-	-	max. 1.00
Inspection Certificate	0.09	0.18	1.06	0.01	0.003	0.036	0.002	0.007	0.03	1.08	0.07	0.11

Table 2.
Mechanical properties of the investigated steel S960MC

	$R_{p0.2}$ [MPa]	R_m [MPa]	$R_{p0.2}/R_m$	A [%]	KV [J]
EN 10149-2	Min. 960	980-1250	-	min. 7	min. 27J / -40°C
Inspection Certificate	1018	1108	0.92	10	-

2.2. Preparation of samples for dilatometric tests

In this research, S960MC steel with 3mm thickness was being investigated. The samples were cut out of sheet in 5 mm wide strips, by laser cutting machine. Since it was not possible to make round bars with a diameter of 4 mm from the experimental material, a prism with a cross section of 4 x 3 mm was chosen, Fig. 1. The prism was cut on a metallographic saw to a final sample length of 10 mm. In order to minimize twisting of the sample due to its heating, it was necessary to make samples with perfect parallel sides of the sample.

Fig. 1 Specimen for dilatometric tests

Dilatometric tests were carried out on a laboratory machine dilatometer DIL 805L, which is located at the Technical University in Liberec. It is a fully automatic hardening dilatometer. The maximum possible achievable temperature is 1500°C and in the "below zero" mode it is possible to set the ambient temperature to -100°C. The test environment can be air, vacuum or a special gas atmosphere (helium - He, argon - Ar, nitrogen - N). High cooling rates are achieved using He. They were performed on 8 different cooling rates, from the slowest one 0.03°C/s to the fastest 100°C/s. The heating rate of 1°C/s and the exposure to the peak temperature (1100°C for 30 s) were equally for all specimens. Whole process was performed in vacuum chamber with 10^{-4} Pa vacuum.

3. Results

Dilatometric tests, determination of transformation temperature, hardness measurement and microstructure analysis were performed on investigated steel.

3.1. Dilatometric tests

Fig. 2 represent the example of complete cycle for dilatometric curve recorded for 1°C/s cooling rate. The transformation temperatures A_{c1} = 769°C and A_{c3} = 855°C are marked on it. Since the conditions in the heating phase were the same, all investigated samples had the same behaviour and shape of dilatometric curve in this phase. The dilatometric curves differed in the cooling section because the cooling rate was variable. The cooling part of the dilatometric curves for all cooling rates are shown in Fig. 3 and Fig 4.

The method of three tanget and first derivation of dilatometric curve (only cooling part) were used to evaluate T1 (start phase transformation temperature) and T2 (finish phase transformation temperature). The same method of analysis was used by the authors in [23, 24] for other types of steel. These methods are graphically explained in Fig. 5 and Fig. 6. Mentioned methods were used for all the 8 different cooling rates. The results of both

methods were compared between themself, and the difference was less than 2%, what represents valuable results.
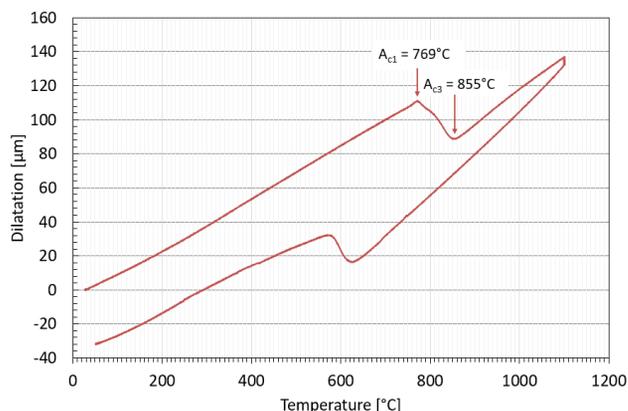

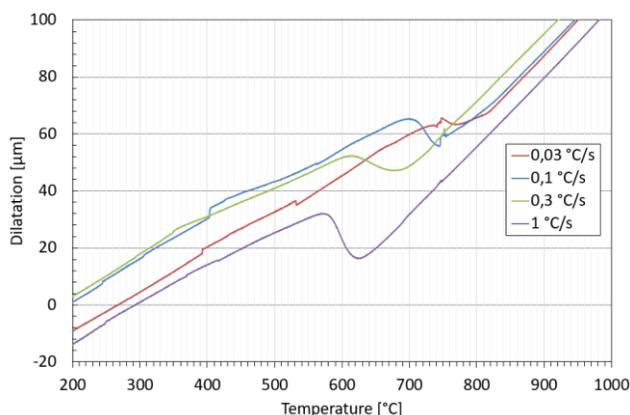Fig. 2 Complete cycle of dilatometric curve for 1 °C/s cooling rate

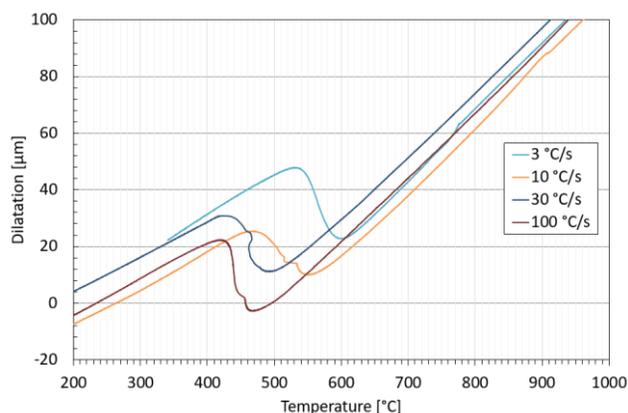Fig. 3 Detail of the dilatometric curve cooling part for rate 0,03°C/s; 0,1°C/s; 0,3°C/s and 1°C/s

Fig. 4 Detail of the dilatometric curve cooling part for rate 3°C/s; 10°C/s; 30°C/s and 100°C/s

The results of the determination of the transformation temperatures are given in the Tab. 3. The dependence of the level

of the transformation temperature T1 and T2 on the cooling rate is graphically shown in Fig. 7.
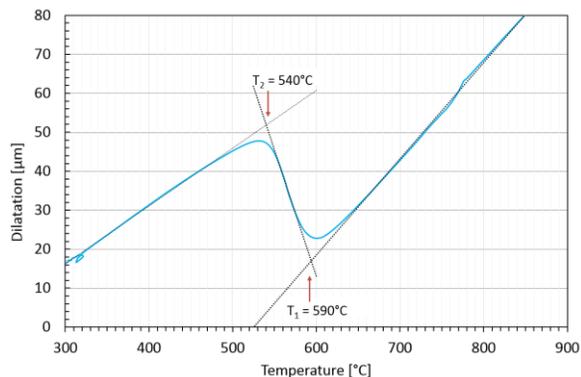

Fig. 5 Determination of the phase transformation temperature according to the three-tangent method (3°C/s cooling rate)
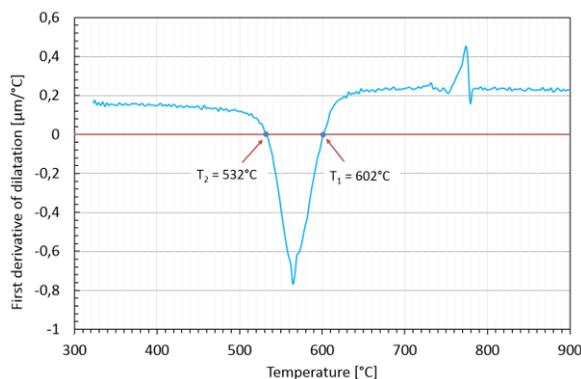

Fig. 6 Determination of the phase transformation temperature according to the first derivative of dilatation (3°C/s cooling rate)

3.2. Hardness of sample

Vickers hardness was measured with a Vickers hardness tester Innovatest Falcon 450. This measurement utilized a load force of 98,07 N for 10 s. The measurement place was on the surface of the cross section through the dilatometric sample. The distance between indentations was 1 mm, there were a total of six indentations. The results of average hardness are listed in the Tab. 4. The standard deviation is also expressed, while the maximum value is reached about 6% at the maximum cooling rate of 100°C/s.

As the cooling rate increases, the hardness increases. The dependence of hardness on cooling rate is exponential (Fig. 8). As can be seen, the type of plot clearly defines the processing–microstructure–property relationship for the steel investigated. Similar conclusions were presented in [21] for high-strength DP (Dual Phases) steel and in [22] for 960MPa grade high strength steel.

The base material has a hardness of 360HV. In the 30°C/s cooling rate where achieved nearly hardness of the base material, it was set as critical cooling rate to reach mechanical properties as base material. A lower cooling rate leads to a reduction in hardness, which will give the material lower strength.
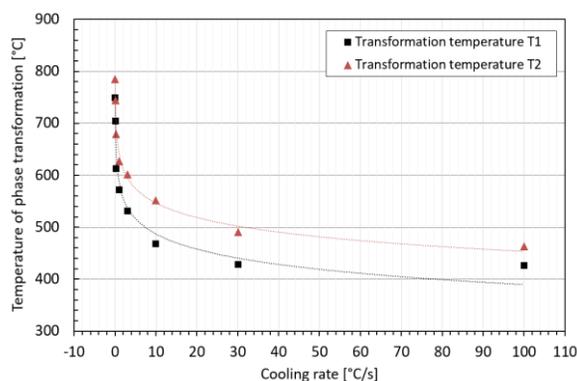

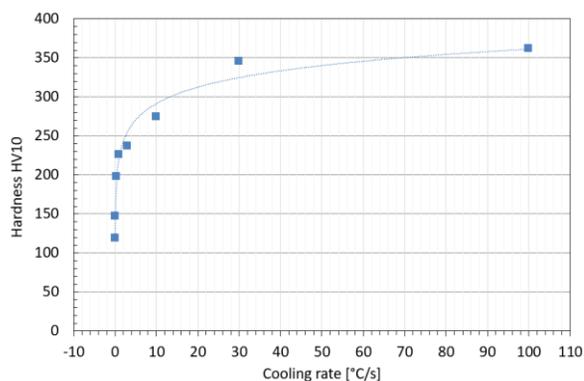Fig. 7 Dependence of the phase change temperature on the cooling rate

Fig. 8 Dependence of the hardness on the cooling rate

Table 3.
Transformation temperatures corresponding to the cooling rates

Method of analyses	Cooling rate [°C/s]	100	30	10	3	1	0,3	0,1	0,03
First derivation	T1/T2 [°C]	463/426	491/429	551/468	602/532	626/571	679/612	744/704	784/749
Three tangents	T1/T2 [°C]	460/428	486/441	550/472	591/539	616/578	691/616	751/702	773/743
	Percentage change for T1 [%]	0,652	1,029	0,182	1,861	1,623	1,737	0,932	1,423
	Percentage change for T2 [%]	0,467	2,721	0,847	1,299	1,211	0,649	0,285	0,808

Table 4.
Hardness HV10 corresponding to the cooling rates

Cooling rate [°C/s]	100	30	10	3	1	0,3	0,1	0,03
Average hardness [HV10]	362	345	275	237	226	198	147	119
Standard deviation [HV10]	5,91	4,77	4,93	2,83	3,01	2,78	4,08	2,72

3.3. Microstructure analysis

Metallographic samples were etched with 2% Nital solution for observing microstructure by an Olympus DSX510 digital optical microscope. The microstructure of base material comprised a mixture of martensite and tempered martensite.

The resulting microstructure is given by the cooling rate. Austenite from a starting temperature of 1100°C is transformed into various decay structures. Fig. 9 documents the resulting microstructures at all cooling rates. At cooling rates of 0.03°C/s to 0.3°C/s, the resulting structure consists of ferrite and perlite. The proportion of perlite increases with increasing cooling rate from about 20% to about 60%. At cooling rate 1°C/s, a bainitic and ferrite phase appears in the microstructure with a ferrite content of about 20%. A similar microstructure was observed at cooling rate 3°C/s. The proportion of ferrite in this case decreases to 15%, at the same time the proportion of bainite increases. At a cooling rate of 10°C/s, the resulting structure is formed by bainite and martensite. At a cooling rate of 30°C/s or more, the microstructure is formed of pure martensite.
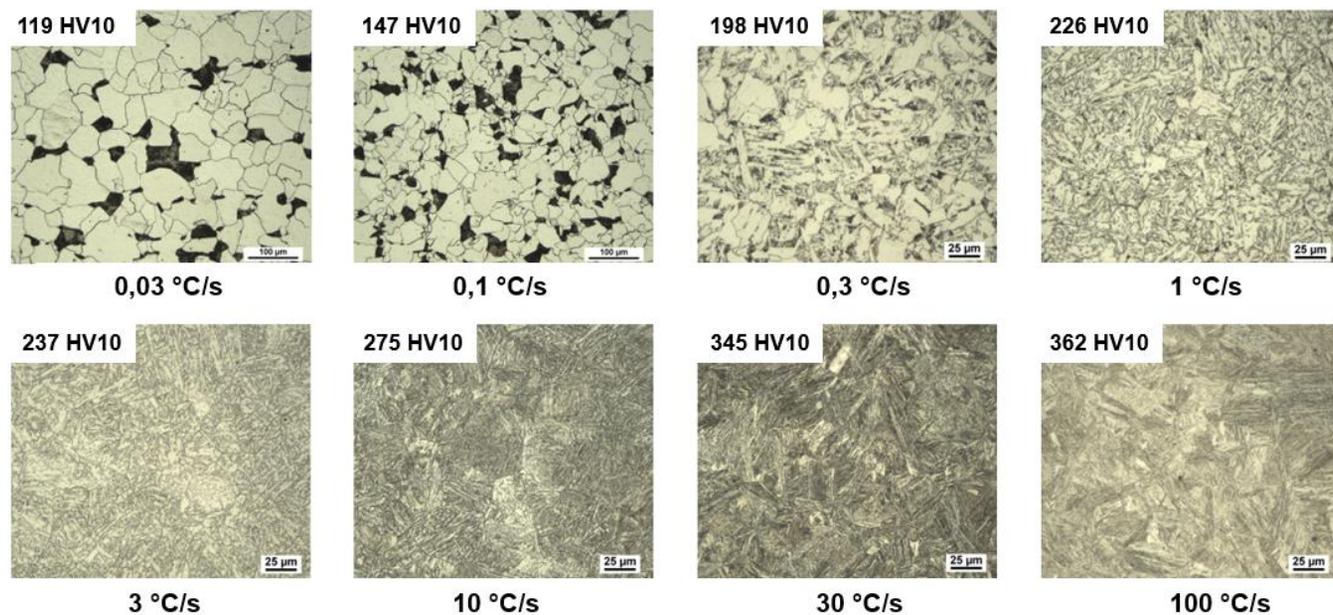

Fig. 9 Microstructures with corresponding cooling rate and hardness

3.4. CCT diagram

The experimental measured data serve to create CCT diagram, which is shown in Fig. 10. Start and finish transformation temperature were plot in the diagram with the axis of temperature and log time. The cooling rate are represented by curves, each is assigned the resulting measured hardness. Based on microstructural and hardness analysis, the structural phases were specified at the diagram. For the cooling rate 100°C/s were measured the highest hardness, which correspond to the 100% martensitic structure. Base material is mixture of bainite, martensite and tempered martensite, which correspond with the cooling rate 30°C/s, where bainite phases can be observed in the structure. Also, the shape of start temperature has rising trend.

At research paper [25] was determined CCT diagrams for S960MC steel. The steel has 8 mm thickness and wt. % of Ni 0,31% higher than in our case. When comparing the two cooling rates, which are identical to our experiment, the hardness in our case was lower by about 30 HV10 (at a cooling rate of 10°C/s) and 11HV10 (at a cooling rate of 10°C/s). This fact is caused by the difference in the chemical composition, especially from the difference in Ni content.

In another study [26], JMatPro software was used to determine CCT diagrams for 8mm thick S700MC and S960QC steels. S960QC has very similar chemical composition as

S960MC steel in our case. For thermal cycle $t_{8/5} = 13s$, which respond approximately to the cooling rate 23°C/s, were bainite start temperature set comparable with our case. For S700MC steel is possible observed big difference in shape and transformation starts temperatures. S700MC contains small amount of Cr and higher amount of Ti. These main differences caused the changes

at the shape of CCT diagrams. To achieve 100% martensite structure for this steel is almost impossible. Based on these knowledge, the small difference in the chemical composition and method of material processing (Q or M) caused significant difference on the CCT diagram shape.
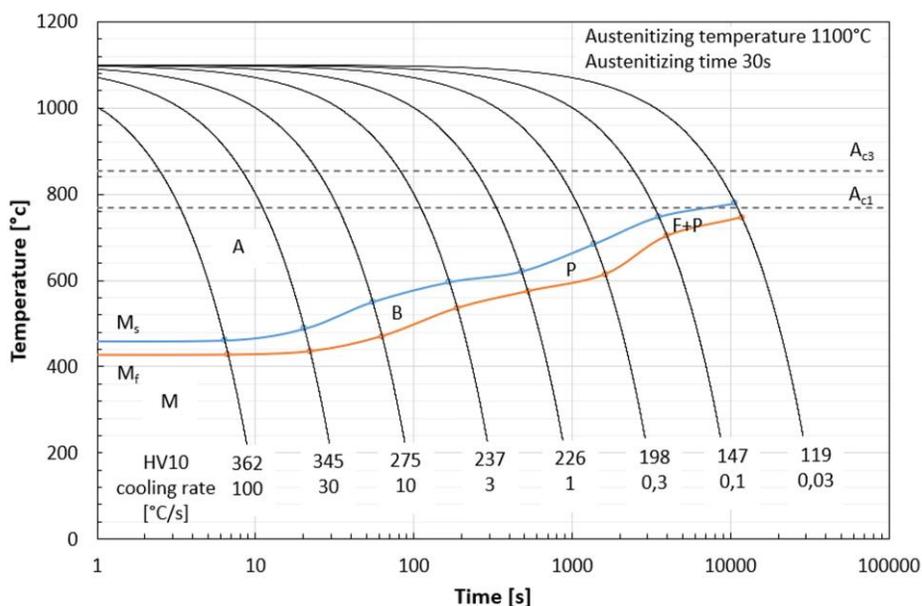

Fig. 10. CCT diagram for S960MC steel with 3 mm thickness

4. Conclusions

The aim of the research was dilatometric analysis performed on the S960MC steel, allowed to investigate changes of microstructure, and set up transformation temperatures affected by different cooling rates. Microstructure analysis of the sample was supported by the hardness measurement. Obtained results can be summarized as follows:

- The method of three tangents and the first derivative of the dilatometric curve for the determination of transformation temperatures is equally applicable and gives results with a percentage change up to 2%.
- With the increase of cooling rate, the microstructure has transformed from ferrite+perlitic to ferrite+bainite, and the hardness increased from 119HV to 237HV; when the cooling rate increased from 10°C/s to 30°C/s, the microstructure of high-strength steel mainly consists of bainite and martensite.
- At the cooling rate of 30°C/s the microstructure is formed by martensite and bainite, and the hardness of the structure achieved the value 345 HV, the base material without thermal influence has 360 HV hardness.
- At the cooling rate 100°C/s were recorded slightly increase of hardness to 362HV, where structure was composed only by martensite.

- The chemical composition and and method of material processing (Q or M) has significantly affect to the shape of CCT diagram. The chemical composition and the method of processing the base material (Q or M) significantly affect the shape of the CCT diagram.
- Physical-metallurgical analysis of a specific welded material is significant for reliable results of numerical simulations.

Acknowledgements

References

[1] Jambor, M., Nový, F., Mičian, M., Trsko, L., Bokůvka, O., Pastorek, F., & Harmaniak, D. (2018). Gas metal arc wleding of thermo-mechanically controlled processed S960MC steel thin sheets with different welding parameters. *Communications - Scientific Letters of the University of Žilina.* 20, 29-35. DOI: 10.26552.C.2018.4.29-35.

[2] Gu, Y., Tian, P., Wang, X., Han, X., Liao, B., Xiao, E. Non-isothermal prior austenite grain growth of a high-Nb X100 pipeline steel during a simulated welding heat cycle process. *Materials & Design*. 89, 589-596. DOI: 10.1016/j.matdes.2015.09.039.

[3] Schneider, C., Ernst, W., Schnitzer, R., Staufer, H., Vallant, R., & Enzinger, N. (2018). Welding of S960MC with undermatching filler material. *Weld World*. 62, 801-809. DOI: 10.1007/s40194-018-0570-1.

[4] Porter, D., Laukkanen, A., Nevasmaa, P., Rahka, K., Wallin, K. (2004). Performance of TMCP steel with respect to mechanical properties after cold forming and post-forming heat treatement. *International Journal of Pressure Vessels and Piping*. 81, 867-877. DOI: 10.1016/j.ijpvp.2004.07.006.

[5] Kik, T., Górka, J., Kotarska, A. & Poloczek, T. (2020). Numerical verification of tests on the influence of the imposed thermal cycles on the structure and properties of the S700MC heat-affected zone. *Metals*. 10, 974. DOI: 10.3390/met10070974.

[6] Mičian, M., Harmaniak, D., Nový, F., Winczek, J., Moravec, J. & Trško, L. (2020). Effect of the t8/5 cooling time on the properties of S960MC steel in the HAZ of welded joints evaluated by thermal physical simulation. *Metals*. 10(2), 229. DOI: 10.3390/met10020229.

[7] Górka, J., Janicki, D., Fidali, M., & Jamrozik, W. (2017). Thermographic assessment of the HAZ properties and structure of thermomechanically treated steel. *International Journal of Thermophysics*. 38, 183-203. DOI: 10.1007/s10765-017-2320-9.

[8] Gomez, M., Vales, P., & Medina S.F. (2011). Evolution of microstructure and precipitation state during thermomechanical processing of a X80 microalloyed steel. *Materials Science and Engineering: A*. 528, 4761-4773. DOI: 10.1016/j.msea.2011.02.087.

[9] Qiang, X., Bijlaard, F.S.K., & Kolstein, H., (2013) Post-fire performance of very high strength steel S960. *Journal of Constructional Steel Research*. 80, 235-242. DOI: 10.1016/.jcsr.2012.09.002.

[10] Moon, A.P., Balasubramaniam, R., & Panda, B. (2010) Hydrogen embrittlement of microalloyed rail steels. *Materials Science and Engineering: A*. 527, 3259-3263. DOI: 10.1016/j.msea.2010.02.013.

[11] Zhao, J., Jiang, Z., Kim, J. S., and Lee, C. S. (2013). Effects of tungsten on continuous cooling transformation characteristic of microalloyed steels. *Materials and Design*. 49, 252-258. DOI: 10.1016/j.matdes.2013.01.056.

[12] Villalobos, J.C., Del-Pozo, A., Campillo, B., Mayen, J., Serna, S. Microalloyed steels trough history until 2018: Review of chemical composition, processing and Hydrogen service. *Metals*. 8, 1-49. DOI: 10.3390/met8050351.

[13] Krauss, G. (2015). *Steels: processing, structure and performance*. Ohio, ASM International. Available on the Internet: https://www.asminternational.org/documents/10192/0/05441G_TOC+%282%29.pdf/82ee161b-e171-9960-caab-74619423b6a4.

[14] Fonda, R. W., Vandermeer, R. A., & Spanos, G. (1998). Continuous Cooling Transformation (CCT) Diagrams for advanced navy welding consumables. *Naval Research Laboratory, United States Navy*. DOI: NRL/MR/6324—98-8185

[15] Kawulok, P., Kawulok, R., & Rusz, S. (2017). *Methodology of compiling decay diagrams of the CCT and DCCT type (i.e. also with regard to the influence of previous deformation (in Czech)*, Retrieved October 10, 2020. Available on the Internet:
https://www.fmt.vsb.cz/export/sites/fmt/633/cs/studium/navody-k-cviceni/deformacni-chovani-materialu/cviceni-12/Doc/cv12.pdf.

[16] Moravec, J., Novakova, I., Sobotka, J. et al. (2019). Determination of grain growth kinetics and assessment of welding effect on properties of S700MC steel in the HAZ of welded joints. *Metals*. 9(6). DOI: 10.3390/met9060707.

[17] Palček, P., Hadzima, B., Chalupová, M. (2004). *Experimental methods in engineering materials (in Slovak)* Žilina, EDIS ŽU Žilina, ISBN 80-8070-179-2.

[18] Pawlowski, B., Bala, P. & Dziurka, P. (2014). Improper interpretation of dilatometric data for cooling transformation in steels. *Archives of Metallurgy and Materials*. 59(3), 1159-1161. DOI: 10.2478/amm-2014-0202.

[19] Herath, D., Mendez, P.F., Kamyabi-Gol, A. (2017). A comparison of common and new methods to determine martensite start temperature using a dilatometer. *Canadian Metallurgical Quarterly*. 56, 85-93. DOI: 10.1080/00084433.2016.1267903.

[20] Vondráček, J. (2013) *Influence of heating and cooling rate on transformational changes of material (in Czech)*, Bachelor thesis, Technical University of Liberec, Czech Republic. Available on the Internet: https://dspace.tul.cz/bitstream/handle/15240/153925/Bakalarska_prace_Vliv_rychlosti_ohrevu_a_ochlazovani_na_transformacni_zmeny_materialu_Jiri_Vondracek.pdf?sequence=1.

[21] Bräutigam–Matus, K., Altamirano, G., Salinas, A., Flores, A. & Goodwin, F. (2018). Experimental Determination of Continuous Cooling Transformation (CCT) Diagrams for Dual-Phase Steels from the Intercritical Temperature Range. *Metals*. 8, 674. https://doi.org/10.3390/met8090674.

[22] Yang, X., Yu, W., Tang, D., Shi, J., Li, Y., Fan, J., Mei, D., & Du, Q. (2020). Effect of cooling rate and austenite deformation on hardness and microstructure of 960MPa high strength steel. *Science and Engineering of Composite Materials*. 27(1), 415-423. DOI: https://doi.org/10.1515/secm-2020-0045.

[23] Pawłowski, B., Bała, P. & Dziurka, R. (2014). Improper interpretation of dilatometric data for cooling transformation in steels. *Archives of Metallurgy and Materials*. 59(3). DOI: 10.2478/amm-2014-0202.

[24] Motyčka, P., Kovér, M. (2012). Evaluation methods of dilatometer curves of phase transformations. In COMAT 2012, 2nd International Conference on Recent Trends in Structural Materials, 21-22 November 2012, Plzeň, Czech Republic, Recent trends in structural materials. Available on the Internet: http://comat2012.tanger.cz/files/proceedings/11/reports/1237.pdf.

[25] Ghafouri, M., Ahn, J., Mourujärvi, J., Björk, T., Larkiola, J. (2020) Finite element simulation of welding distortions in ultra-high strength steel S960 MC including comprehensive

thermal and solid-state phase transformation models, *Engineering Structures.* 219, DOI: 10.1016/j.engstruct.2020.110804.

[26] Bayock, F.N., Kah, P., Mvola, B., Layus, P. (2019). Effect of heat input and undermatched filler wire on the microstructure and mechanical properties of dissimilar S700MC/S960QC high-strength steels. *Metals. (9).* DOI: 10.3390/met9080883.